Complete experimental performance characterisation of 13X for domestic thermochemical energy storage applications using a novel high-pressure DSC system

Daniel Mahon [1,*] and Philip Eames [1]

[1]   Centre for Renewable Energy Systems Technology (CREST), School of Mechanical, Electrical and Manufacturing Engineering, Loughborough University, Loughborough, LE11 3TU, UK 1; d.mahon@lboro.ac.uk
*Corresponding author. Email: d.mahon@lboro.ac.uk

ABSTRACT

One problem with utilising solar renewable energy sources, for domestic space heating and domestic hot water in the UK is the mismatch between energy supply and energy demand due to the seasonal variation. One way to mitigate this phenomenon is to utilise seasonal thermochemical heat storage. 13X molecular sieves have received recent attention as a thermochemical energy storage material for domestic use due to the heat stored when dehydrated and released when rehydrated. Minimal attention has been paid to the dehydration conditions and the impact this has on the heat release from dehydrated 13X. The reported study experimentally characterised the charge and discharge enthalpy of 13X molecular sieves using a custom designed novel Differential-Scanning-Calorimeter apparatus and Thermogravimetric-Analyser for mass loss investigations. This study shows how employing different thermal analysis testing methodologies can produce different results. The impact that the grade of nitrogen employed has on the mass change of the 13X samples, and the length of time exposed to the nitrogen purge as the charged sample cools, can have a dramatic impact on the mass of the 13X sample. When using a nitrogen generator or technical grade nitrogen as the purge gas in the cooling phase after a 500 °C dehydration, (charging), the mass of the 13X sample increased by 13 % and 17 %, respectively, this could potentially impact the later adsorption potential leading to reduced hydration and energy output on discharge. The hydration enthalpy (energy output) of 13X for varying charge (60–150 °C) and discharge (25–60 °C) temperatures, with a discharging partial vapour pressure (pH_2O) of 0.64 kPa are also presented. This work provides reference values for the expected energy output from 13X for a range of charge and discharge temperatures, for example, showing that the energy output varies from 660-500 J/g with different discharge temperatures if the sensible heat is not utilised.

Keywords: thermochemical energy storage, thermal energy storage, interseasonal storage, domestic space heating, molecular sieves, 13X, long duration energy storage, thermal analysis, TGA and DSC, climate change.

1. INTRODUCTION

For the 5 years (2015 – 2019 inclusive), the percentage of the UK's total energy consumption used for Domestic Space Heating (DSH) plus Domestic Hot Water (DHW) was 28.9%, calculated from the National Statistics : Energy consumption in the UK [1]. Using the same data source, the average percentage of DSH plus DHW energy sourced from gas and oil was 68.7%. These two percentages are shown in Figure 1 to be consistent since 1970 and 1990 for the total energy consumption and energy sourced from gas and oil, respectively. Hence, on average for 2015 – 2019 19.8% of the total UK's energy consumption was sourced from gas and oil for DSH plus DHW. If the UK is to reach its new targets of a 78% emissions reduction by 2035 [2] and to be net zero by 2050 [3] the energy for DSH and DHW will need to be delivered from energy sources which do not emit Green House Gases (GHG's).
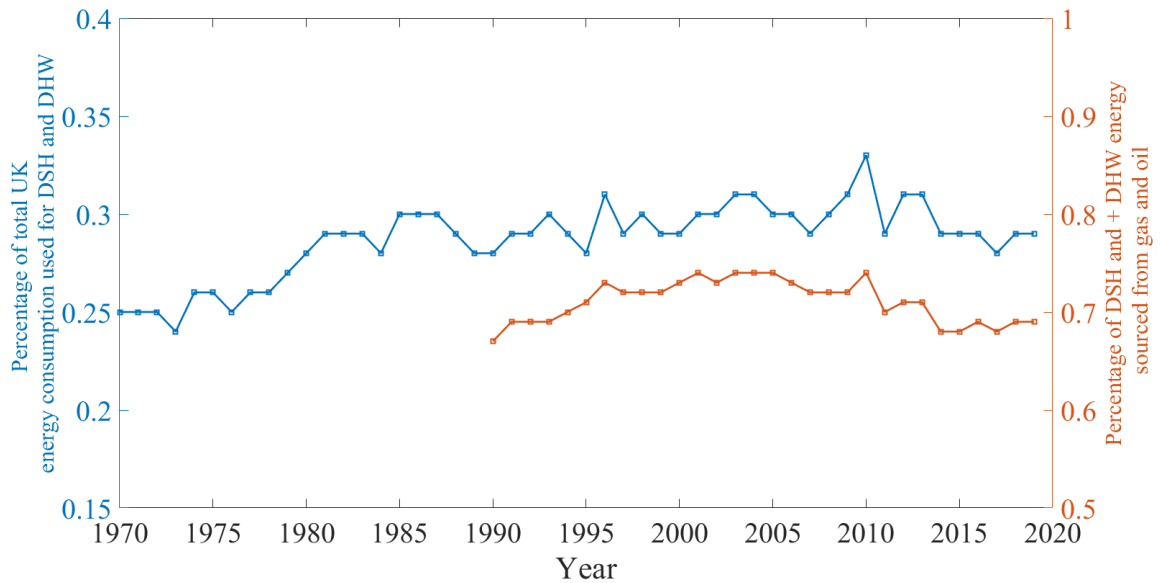
Figure 1 Percentage of DSH + DHW energy sourced from gas and oil in the UK (orange plot), Percentage of UK total energy consumption used for DSH + DHW (blue plot) (data generated using National Statistics: Energy consumption in the UK [1])
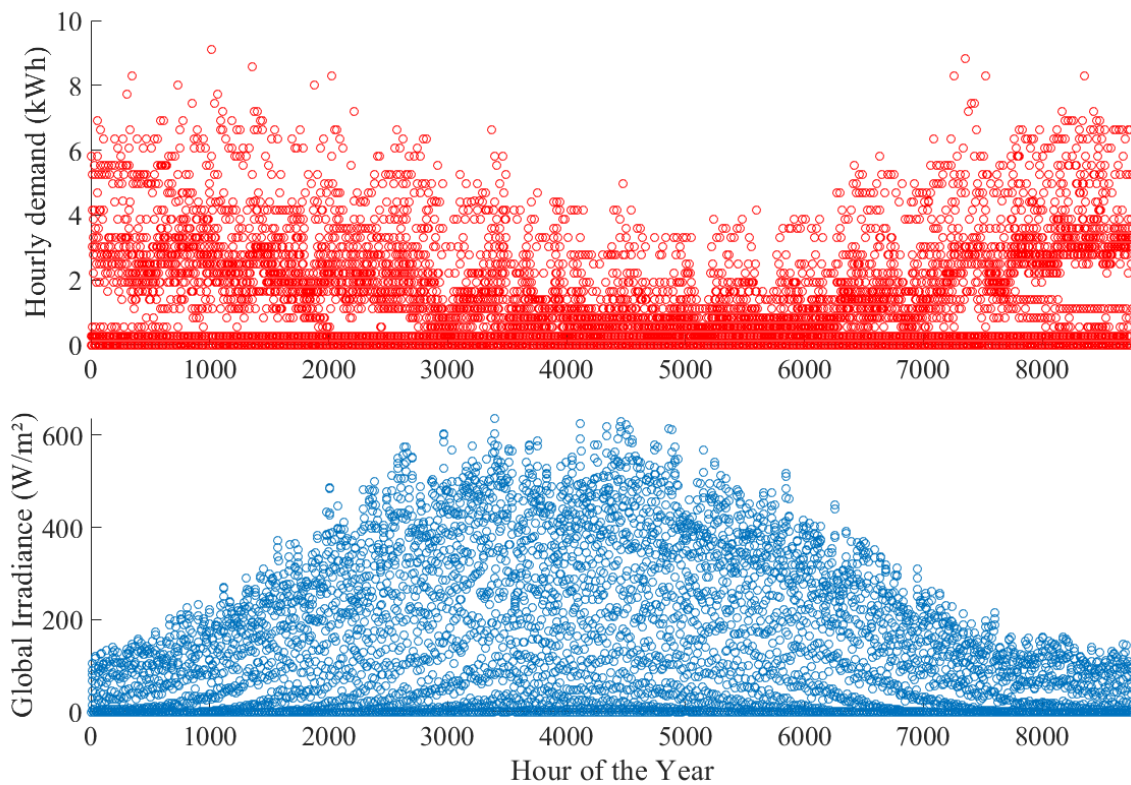

Figure 2 Measured hourly demand for a UK dwelling (top red plot) (plot generated from source [4]), Average measured global irradiance (bottom blue plot) (plot generated from source [5]).

One problem with sourcing energy for DSH and DHW in the UK from solar renewable energy sources is the mismatch between energy supply and energy demand due to the seasonal variation. This means that the UK receives the highest amount of solar radiation when the demand is the lowest, hence, in the summer months. This is illustrated in Figure 2 which shows the measured demand for a UK dwelling (top red plot) (data for plot sourced from [4]) and average measured global irradiance at a location in Sutton Bonington, Nottinghamshire, UK (bottom blue plot) (data for plot sourced from [5]) which is in the centre of England.

This means that the excess energy, which could be converted into thermal energy utilising a Solar Thermal Collector (STC), in the summer months is wasted or additional energy is used to cool dwellings which have become overheated due to excess solar gains (i.e. for example, through air conditioning). One way to take advantage of this mismatch between supply and demand is to store the unutilised solar radiation in the summer months and release this stored energy in the winter months when demand is high, and supply is low. This can be achieved with seasonal Thermal Energy Storage (TES). There are three main types of TES, Sensible Thermal Energy Storage (STES), Latent Thermal Energy Storage (LTES) and Thermochemical Energy Storage (TCES). STES utilises the specific heat capacity of a substance and stores heat by heating a material up and when thermal energy is required the heat is extracted from the material causing the material to cool. This is the principal behind a domestic hot water tank, the water in the tank is heated to store thermal energy then, when there is a need for hot water (i.e. to flow through radiators to heat the dwelling or for use in a shower or bath) heat can be extracted from the water as the water cools. Water used for DSH is able to store around 105 J/g of thermal energy when stored at 65 °C. LTES utilises the specific heat capacity of a material in the same way STES does, however, LTES also takes advantage of the enthalpy involved due to the phase transition of a material. For example, when a paraffin wax, used in a domestic LTES system, is heated to its melting temperature it typically requires around 200 J/g of latent heat to change from a solid wax to liquid wax. If the liquid wax is kept above its melting temperature thermal energy can be stored as sensible heat and also latent heat. When heat is required, it can be extracted from the liquid wax. As the wax cools and crystalises back into a solid it releases the stored latent heat.

When heat is stored in both STES and LTES systems there are parasitic losses through the insulation to the surrounding environment. This makes STES and LTES unsuitable for seasonal heat storage and only short-term (i.e. 24 to 48 hours) TES.

TCES stores thermal energy in the form of chemical potential energy. This means that a thermochemical energy store can be allowed to cool to ambient temperatures and only lose the sensible heat component of its stored energy. For a domestic system this can account for around 20% of the thermal energy input. As long as the reactants are kept separate from one another the chemical potential energy can be stored indefinitely making TCES suitable for inter-seasonal energy storage.

A TCES system for DHW and DSH would typically have a maximum charging temperature of around 150 °C as this is assumed to be on the upper end of what a domestic Vacuum Solar Thermal Collector (VSTC) system can achieve. With a temperature difference of 100 °C (i.e. 120 °C outlet temperature with an ambient temperature of 20 °C) a VSTC can have an efficiency of around 50% [6]. Over the last 10 years there have been many research studies which look at different materials intended to be used as TCES materials for domestic heat storage [7]–[12]. The thermochemical materials proposed for low temperature (i.e. <150 °C charging temperature) thermal energy storage tend to be absorbents (i.e. 13X) [8]–[11] or salt hydrates (i.e. $MgSO_4.7H_2O$, $MgCl_2$) [9]–[11]. It is important for the TCES materials to be safe for use in a domestic environment and typically the TCES material will react with water to release the stored thermal energy.

There have been many published research papers which consider the use of 13X as a TCES material either on its own or as a host matrix to be impregnated with other materials, such as salt hydrates [12] [9]. Some of the studies consider the changing discharging relative humidity[8], [9], [11] and 13X has been tested at a range of different charging temperatures [13].

The research reported investigates the potential of 13X as a TCES material for domestic use. This research also demonstrates the importance of a consistent thermal analysis testing methodology and illustrates how different methodologies can result in different data sets. The work uses a realistic partial vapour pressure for discharging (pH_2O) which has been calculated from measured meteorological data. This work also looks at how the energy output is impacted by the charging and discharging temperature. The results from this work are being used to inform the development of large scale TCES systems for domestic use, as well as being intended to provide reference data on 13X to be used by others and present a methodology for other researchers to use to allow for comparison of experimental research data.

2. RESULTS

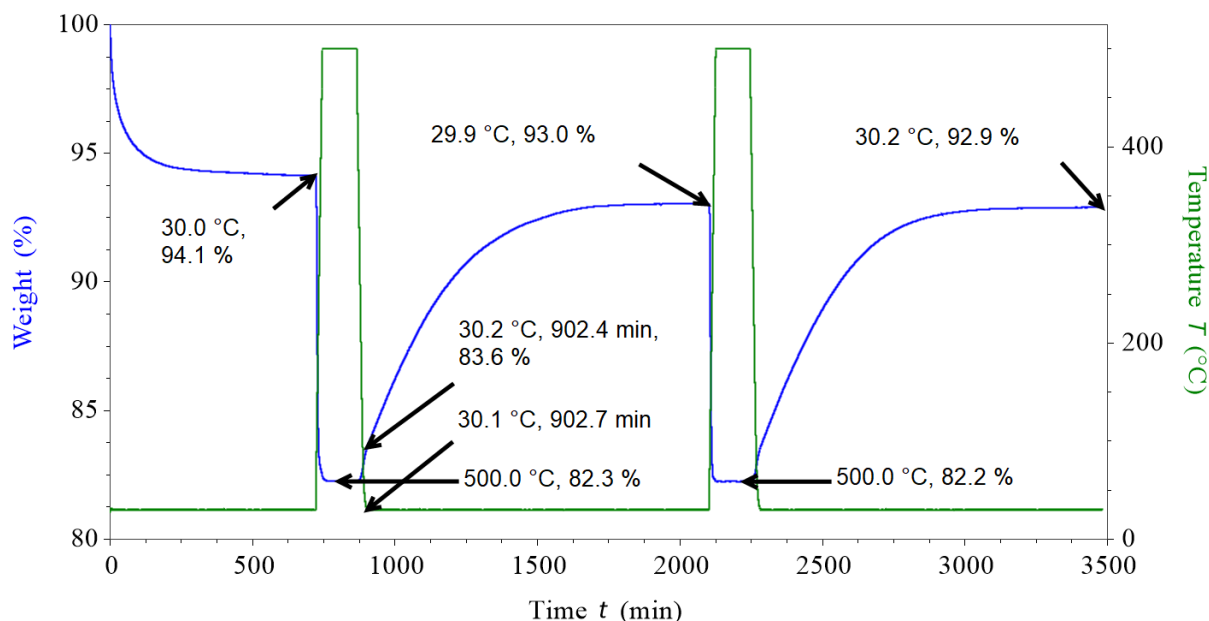### 2.1. Issues with typical 13X DSC and TGA testing methodology

Figure 3 TGA mass change data of a 13X crushed pellet sample as it is heated and cooled between 30 and 500 °C

It is typical for 13X samples and many materials which are investigated for use as domestic TCES materials using thermal analysis equipment, namely ThermoGravimetric Analysis (TGA) and Differential Scanning Calorimetry (DSC), to be heated (charged) to remove the bound moisture under an inert purge gas, which is typically nitrogen or argon. The sample is then cooled while still being purged with an inert purge gas.

Figure 3 shows TGA mass change data for a crushed 13X pellet sample as it was heated and cooled between 30 and 500 °C and purged with nitrogen produced by a nitrogen generator. This figure demonstrates the issue allowing the removal of moisture (dehydration) of 13X to take place under a nitrogen purge gas. The sample gains around 11% of mass as it cools in the nitrogen purge gas. The length of the experiment shown in Figure 3 is around 3500 minutes (58.3 hours or 2.4 days). Annotated on Figure 3 is the time when the sample is cooled from 500 °C to 30 °C (902.7 mins) and the corresponding mass (83.6 %) which is a 1.3% increase from the mass when the sample was at 500 °C. Under normal testing circumstances for domestic TCES research the sample can be cooled from a lower
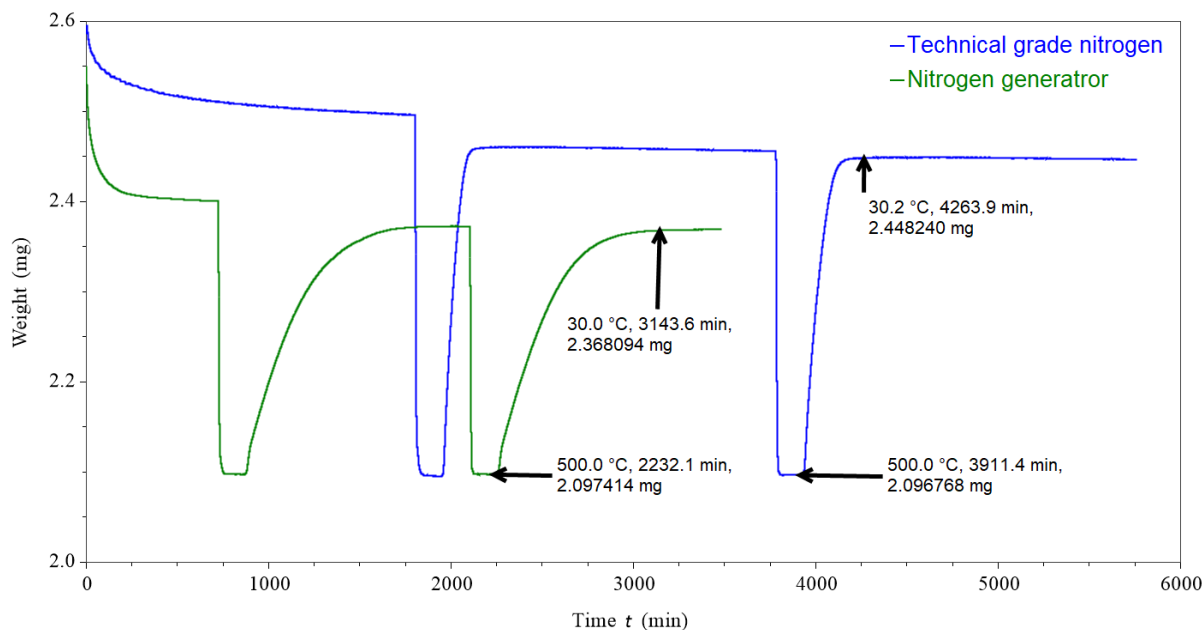

Figure 4 Change in mass of a 13X sample as it is heated and cooled in two different grades of nitrogen purge gas

temperature than 500 °C (i.e. a maximum temperature of around 150 °C is typical) and then once at the cooled temperature, which in this case is 30 °C, it could be exposed to a humid environment to rehydrate the sample. In this hypothetical situation the change in mass would likely be less than 1.3% and therefore, not seen as significant. The change in mass is a function of time. As can be seen in Figure 3 if the sample is given enough time, around 1200 minutes (20 hours), in a nitrogen purge gas the change in mass from 500 °C to 30 °C is 10.7%. Therefore, the mass gain seen for 13X can be different depending on the length of the cool down period which is why it is important to consider this when designing the test methodology or comparing results from different studies.

For comparison Figure 4 shows the same 13X sample as it was heated and cooled in two different grades of nitrogen purge gas. The green and blue plot shows the mass change data as the 13X was heated and cooled with nitrogen from a Peak Scientific Genius 1053 nitrogen generator (purity up to 99.995%, please note this is an up to value quoted by the manufacturer) and technical grade nitrogen (99.999%), respectively. The mass of the 13X sample after the first heating cycle to 500 °C was the same for each test (both tests have a sample mass of 2.097 mg). When the samples were cooled the rate of change of mass was different depending on the nitrogen used. For the nitrogen generator the sample gained around 13% mass in 912 minutes (~15.2 hours), when technical grade nitrogen was used the change in mass was 17% in 353 minutes (~5.9 hours). When a technical grade nitrogen (99.995%) was used the 13X sample was able to increase in mass by 17% in 5.9 hours which is a larger mass change and a quicker rate than when the sample was cooled in nitrogen produced by a nitrogen generator. This demonstrates the importance of

considering the cooling purge gas and the cooling periods, including isothermal periods, used when testing an absorbent material. Different grades of purge gas and different isothermal periods at the cooled temperature (i.e. 30 °C in this case) can all change the mass of the sample and impact the results.

3.2mm 13X pellets crushed into a powder using a mortar and pestle and 13X fine power were tested in the TGA, the data generated can be seen in Figure 5. The data was normalised to the mass at the first 500 °C cycle and the mass for the generator cycles (i.e. at the first 500 °C isotherm for the nitrogen generator cycle the mass was normalised to 1). Hence, all of the powder plots were normalised on the mass at the first 500 °C for the 'Powder - Generator' mass point. Both powder and both pellet samples had the same mass at the 500 °C point. This is important as they were the same sample, but it means that they were dehydrated (regenerated) to the same point because the absolute mass in mg was the same in the TGA. From figure 5 it can be seen that the powder samples gained more mass than the corresponding pellet samples. This is likely to be because the pellet samples included material used to form the pellets which is less reactive than the pure 13X powder. Both the powder and the pellet samples gained more mass when purged with technical grade nitrogen. The mass gain differential for the powder and pellet samples between the nitrogen generator and technical grade nitrogen was ~4% for both. The starting mass, when the samples had been exposed to the ambient, for each of the samples was higher than the mass gain after the nitrogen purge.

This clearly illustrates the importance of considering the methodology adopted for testing absorbent materials and the purge gas used in the testing. Changing the purge gas and the length of time the absorbent is
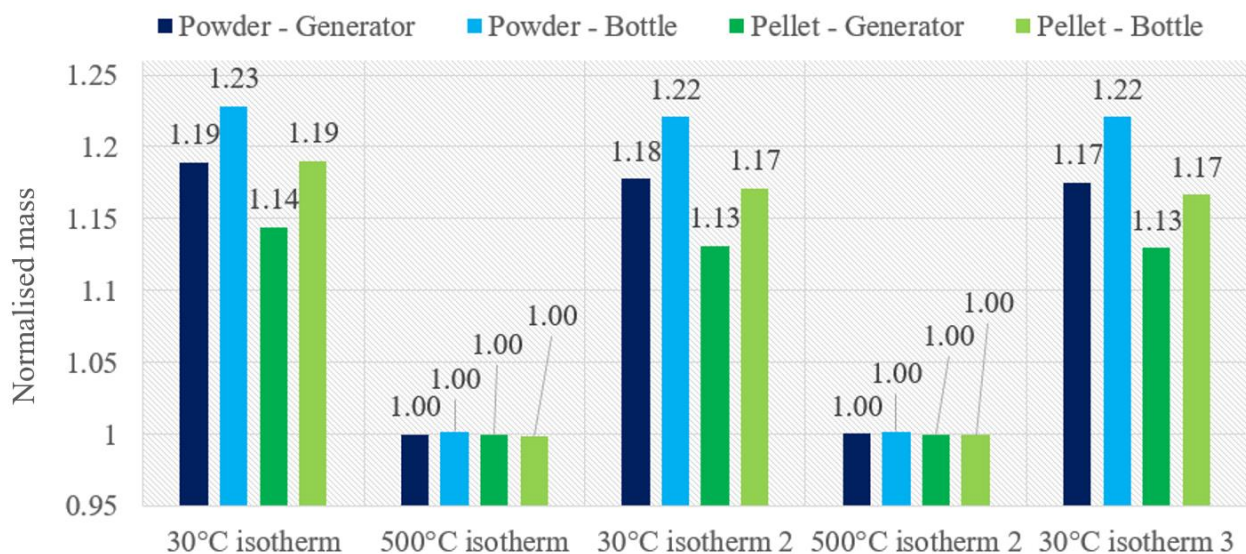

Figure 5 Change in mass of 13X samples as they are heated and cooled in different purity nitrogen purge gas.

exposed to the purge gas can have an impact on the mass gain of the absorbent. This means that identical testing methodologies which only have a difference in the grade of the nitrogen purge gas used, can produce different mass change results. Or identical methodologies which only change the length of time the absorbent is held at the lower cool temperature could produce different mass change results.

2.2. High pressure (DSC25p) DSC tests

The mass gain seen in the cool down period when 13X was purged with nitrogen (see Figure 3 and Figure 4) is important as this means the samples were absorbing gas when they were cooling from there charging temperature. If this was to happen in an actual thermal storage system a significant portion of the energy stored in the charging phase could be released in the cool down phase resulting in less energy being stored for future use. This is the case if the absorbed material (i.e. from the inert purge gas) reduces the sorption potential of the 13X to uptake water and release heat. To address this testing methodology issue, a custom experimental apparatus was attached to a TA Instruments DSC25p high-pressure DSC (pDSC) to allow the system to be evacuated at the charging temperature to remove all gases and then cool down under vacuum. This test ensured that minimal amounts of gas reacted with the TCES sample as it cooled.

2.2.1. Testing 13X using realistic pH₂O conditions to emulate the conditions likely in an open domestic TCES reactor.

Experimental tests were performed with charge/discharge conditions controlled to match those expected in a large-scale domestic system, to understand the realistic potential of 13X. It is expected the TCES materials will be charged in the summer months, using ambient air heated to the required charging temperature and that the TCES material will be discharged in the winter months, with ambient air.

Met office recorded data [5] was used to calculate the average pH_2O for the last 10 years of data recorded at the Sutton Bonington, Nottinghamshire location, in the East Midlands region of the UK. The calculated average value for pH_2O for the winter months was 0.66 kPa. A commonly used temperature and pH_2O for TCES testing is 20 °C at 56% RH (1.3 kPa pH_2O) [14]. This research assessed the energy output data from 13X using realistic ambient air pH_2O (i.e. 0.66 kPa) for different charging and discharging temperatures.

Figure 6 shows the DSC25p measurement data from a 13X charge and discharge cycle. The first step in the experimental procedure was purging the TCES sample with dry N_2 gas (technical grade). This process can induce an endothermic heat flow as it dries the sample,

which is evident at point 1 on Figure 6. Of the three tests performed, test C (red plot) had a larger endothermic heat flow at point 1 compared to tests A and B. This was because the sample had more adsorbed water when test C was conducted compared to when tests A or B were conducted. At the start of test B the sample had only previously been hydrated with the average winter pH_2O (0.64 kPa) (i.e. slightly lower than the calculated average winter pH_2O of 0.66 kPa). When test C started the sample had been previously hydrated with 1.3 kPa pH_2O and was more hydrated than when test B commenced. Due to the greater hydration level the N_2 purge at the start of test C (labelled number 1 on Figure 6) produced a larger endothermic heat flow than test A or B. This indicates that the TCES material in test C had more loosely bound water than tests A or B, suggesting that higher values of pH_2O results in more water being absorbed, but part of the extra water absorbed is loosely bound.

After the N_2 purge phase was complete the samples were heated to the charging set point temperature of 150 °C. All three tests (A, B and C) had a dehydration enthalpy (excluding the N_2 purge contribution) of 778 J/g, 772 J/g and 782 J/g. These values are all within 1% of each other indicating that the additional water absorbed by the 13X in tests B and C was removed by the N_2 purge gas before the heating of the sample commenced.

In test D, shown in Figure 6, N_2 with a 1.3 kPa pH_2O was used to dehydrate the 13X sample. Point 3 on Figure 6 is the point when the vacuum pump was switched on to remove gas from the DSC before the sample was cooled. For tests A, B and C there was only a slight change in the heat flow when the vacuum pump was switched on. For test D the vacuum pump resulted in an endothermic heat flow peak with an enthalpy of 106 J/g. This indicates that the vacuum pump did not remove any or a minimal amount of water for tests A, B or C but removed a significant amount of water for test D. This is an important finding as test D was the test in which the 13X was hydrated with nitrogen that had a water content similar to that which ambient air could have. The average partial vapour pressure of summer ambient air calculated from the weather data for Sutton Bonnington, Nottinghamshire, UK is 1.16 kPa. Test D was conducted with air with a pH_2O of 1.3 kPa. The vacuum pump was used in the test procedure to ensure that minimal gas was present to react with the samples during the cooling phase, the importance of which was previously demonstrated (see Figure 3 and Figure 4). The vacuum was not used to further dehydrate the sample. If 1.3 kPa pH_2O air was used to dehydrate 13X in a large-scale system and a vacuum pump was not used it is likely that around 106 J/g of energy would be lost.
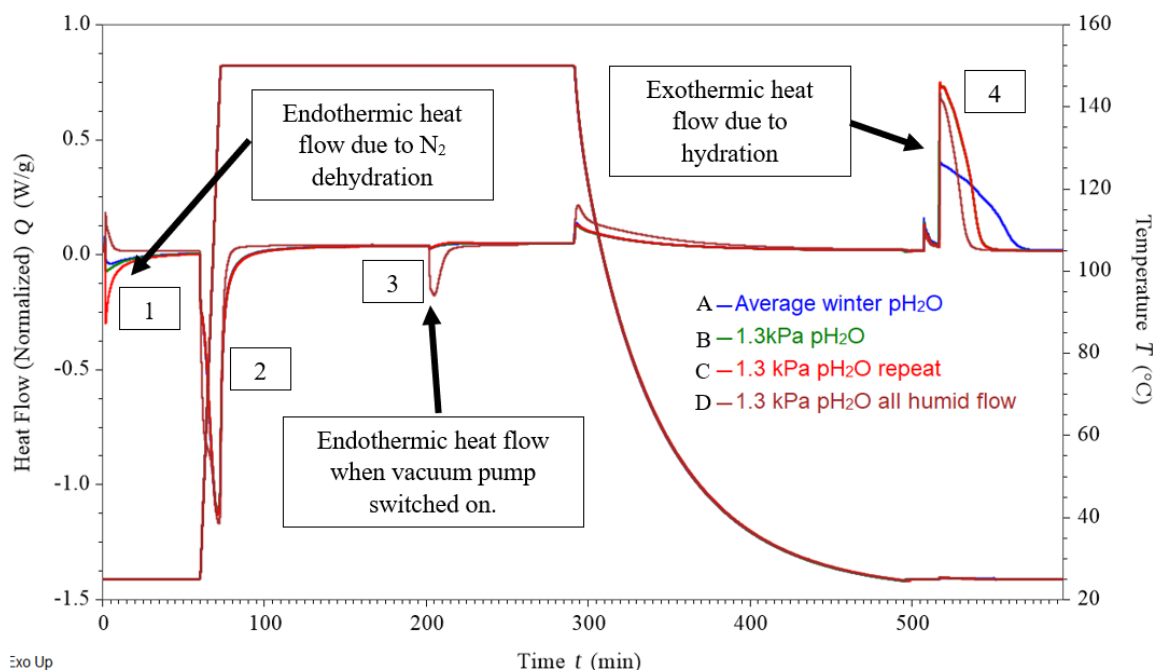
Figure 6 DSC charge and discharge data for 13X with different pH$_2$O values.

Once the sample had been evacuated at the charging temperature the sample was cooled to the hydration temperature, in this test 25 °C, while under vacuum. The hydration section is labelled as number 4 in Figure 6. Tests B and C, had a peak hydration heat of ~0.74 W/g, test A and test D had a peak hydration heat of ~0.4 W/g and ~0.7 W/g, respectively. Tests B, C and D all have a similar peak hydration heat with test D having a slightly smaller value. The hydration enthalpy for tests A, B, C and D are 711 J/g, 762 J/g, 759 J/g and 456 J/g, respectively showing that the energy output from the 13X is reduced when dehydrated with a 1.3 kPa pH$_2$O purge gas, compared to dry purge gas, even when a vacuum pump is used to remove any gas from the system at the charging temperature.

2.2.2. Impact of charging and discharging temperature on the energy output of 13X

The DSC25p custom setup was used to investigate the energy output from 13X for a range of different charge and discharge temperatures and the corresponding energy outputs measured. This comprehensive data can be used to help design and develop large scale 13X based TCES systems.

For these experiments 13X pellets were used as they were supplied (3.2mm pellets) since this is the most likely form that would be used in a large scale TCES system. The experimental procedure followed was the same as presented in Figure 6 except the charge and discharge temperatures were varied. The samples were dehydrated using a dry nitrogen purge. After the

evacuation at the charging temperature, the sample was allowed to cool to 25 °C. The DSC25p was not equipped with any forced cooling and only lost heat to the surrounding environment, the lowest hydration temperature tested was 25 °C. The sample was then heated from 25 °C to the initial discharge temperature (40 °C or 60°C). As the sample was heated the sensible heat required for heating the sample from 25 °C to the initial discharge temperature was measured.

When at the initial discharge temperature (i.e. 40 °C or 60°C) the TCES sample was first repressurised to atmospheric pressure using a pure N$_2$ purge gas, to ensure that none of the water in the solvent tank was exposed to the low pressures of the DSC. This re-pressurisation typically took 8 minutes. Once at atmospheric pressure the hydration (discharge) reaction took place using a 0.64 kPa pH$_2$O (the average winter pH$_2$O value). Once hydration at the discharge temperature was complete the sample was cooled back to 25 °C while still being exposed to a humid air stream. As the sample cooled it was able to absorb more moisture and release more energy defined as the 'cool down enthalpy'. Some of the cool down enthalpy measured as the sample cooled was the sensible enthalpy of the sample. The sensible enthalpy was subtracted from the cool down enthalpy, which is a combination of the sensible enthalpy and the hydration enthalpy, this gave the cool down hydration enthalpy of the sample.

The resultant enthalpy is defined as the hydration enthalpy minus the sensible heat of the sample. If used for an application where heat below the hydration
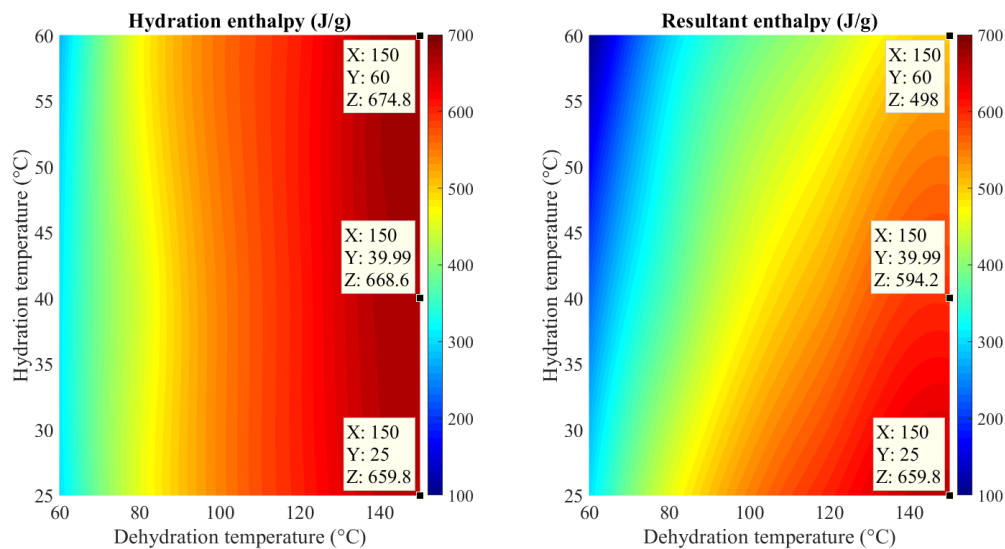
Figure 7 Hydration enthalpy and resultant enthalpy from 13X after dehydration in dry N_2 and hydration at 0.64 kPa (average winter pH_2O) with different combinations of hydration and dehydration temperatures. The 13X was tested as a formed pellet.

temperature (i.e. 40 or 60 °C) is not useful then the sensible heat input to the material to raise its temperature to the hydration temperature would be wasted energy, therefore this should be subtracted from the hydration enthalpy.

The overall amount of enthalpy released from a TCES system depends on the hydration temperature and if energy available below the hydration temperature can be utilised. It also depends on the dehydration temperature of the system and on the ambient temperature of the material in the system. For example, if a system when operated i) maintains the TCES material temperature at 40 °C, ii) utilises the hydration enthalpy at 40 °C and, iii) once hydrated the material is kept at 40 °C then there are no additional sensible losses in the hydration process as the material does not have to be heated to its useful hydration temperature (40 °C). This system would also have a lower dehydration enthalpy than a system which was allowed to cool from 40 °C to ambient (i.e. 25 °C) after the hydration as the material would not absorb water in the cool down phase from 40 to 25 °C, as it is kept at 40 °C. This system would have a lower hydration enthalpy compared to a system with a lower hydration temperature (for example 25 °C) as water would be absorbed when the sample cooled from 40 to 25 °C.

Figure 7 is an experimentally derived surface plot of the hydration enthalpy and resultant enthalpy for 13X when it is hydrated with 0.64 kPa (average winter pH_2O) and dehydrated using a dry N_2 gas. The hydration enthalpy plot shows all of the hydration enthalpy from the initial hydration temperature (i.e. 40 °C, 60 °C) and the cool down enthalpy but removes the sensible enthalpy from the initial hydration temperature back to 25 °C, as this heat flow includes both the cool down

hydration enthalpy and the cool down sensible enthalpy. If the system can make use of any heat above ambient (i.e. 25 °C in this case) then all of the hydration enthalpy can be utilised and there is no waste of sensible heat as it will be recovered on the cool down phase. The resultant enthalpy is the hydration enthalpy for the initial hydration temperature minus the sensible enthalpy for heating the sample from 25 °C to the initial hydration temperature (i.e. 40 °C or 60 °C), in reality this is what would likely happen and it is assumed any heat below the initial hydration temperature is not useful so cannot be recovered when the sample cools back to 25 °C.

Figure 7 shows that the hydration enthalpy is dependent on the dehydration temperature and not the hydration temperature. The resultant enthalpy is dependent on both the hydration and dehydration temperature. The difference between the hydration and resultant enthalpy increases as the hydration temperature increases. This is for two reasons, first as the hydration temperature increases there is more wasted sensible enthalpy in the system and secondly the hydration enthalpy is lower the higher the hydration temperature as the sample is not able to absorb as much moisture under the same conditions. As an example, with hydration and dehydration temperatures of 25 °C and 150 °C the hydration and resultant enthalpy is the same. For hydration and dehydration temperatures of 40 °C and 150 °C the difference is 74 J/g and for hydration and dehydration temperatures of 60 °C and 150 °C the difference is 177 J/g.

Figure 7 is presented as charging temperature against discharge temperature in a surface plot so it is possible to identify the expected hydration enthalpy for any charge and discharge combination within the tested

range (i.e. charge temperature 40 – 150 °C and discharge temperature 25 – 60 °C). The software used (MATLAB) creates a surface of values between the input experimental data which means data is provided for combinations which haven't been experimentally tested.

CONCLUSIONS

13X absorbs a significant amount of gas when it is cooling after a charging process. Measurements showed that an increase in mass of 13 to 22 % results due to gas adsorption throughout the cooling process depending on the structure of the sample and the type of nitrogen purge gas used. The adsorbed gases may occupy the active sites in the material which can result in fewer available sites for water adsorption and subsequent energy release, ultimately reducing the energy output of the material.

This study provides a methodology to overcome the gas adsorption issue by utilising a vacuum pump at the peak charging temperature to remove all gases from around the sample.

This paper provides reference data illustrating the expected energy output from 13X for different charge and discharge temperatures in the form of a surface plot. This plot can be utilised by researchers and design engineers to help design systems utilising 13X without the requirement to conduct their own experiments, ultimately saving time and cost.

AUTHORS' CONTRIBUTIONS

Daniel Mahon – experimentation, data collection and analysis, paper writing and editing. Philip Eames – paper editing, obtained funding for all three projects to be conducted, and guided all three projects.

ACKNOWLEDGMENTS

REFERENCES

[1] UK_Government, "National Stastics: Energy consumption in the UK," 2021. https://www.gov.uk/government/statistics/energy-consumption-in-the-uk (accessed May 18, 2021).

[2] UK_Government, "UK enshrines new target in law to slash emission by 78% by 2035," 2021. https://www.gov.uk/government/news/uk-enshrines-new-target-in-law-to-slash-emissions-by-78-by-2035#:~:text=The Prime Minister will urge,to align with net zero.&text=The UK is leading the,future is now in sight.

[3] DBE&IS, "UK becomes first majour economy to pass net zero emissions law," 2019. https://www.gov.uk/government/news/uk-becomes-first-major-economy-to-pass-net-zero-emissions-law (accessed Feb. 26, 2021).

[4] Building-Research-Establishment-(BRE), "Milton Keynes Energy Park Dwelling 1990," UKERC, 1990. https://data.ukedc.rl.ac.uk/browse/edc/efficiency/residential/Buildings/MiltonKeynesEnergyPark_1990

[5] UK_Met_Office, "Met Office (2006): MIDAS: Global Radiation Observations. NCAS British Atmospheric Data Centre," 2018. http://catalogue.ceda.ac.uk/uuid/b4c028814a666a651f52f2b37a97c7c7

[6] D. Mahon, P. Henshall, G. Claudio, and P. Eames, "Feasibility study of MgSO 4 + zeolite based composite thermochemical energy stores charged by vacuum flat plate solar thermal collectors for seasonal thermal energy storage," Renew. Energy, vol. 145, pp. 1799–1807, 2020, doi: https://doi.org/10.1016/j.renene.2019.05.135.

[7] S. Z. Xu, Lemington, R. Z. Wang, L. W. Wang, and J. Zhu, "A zeolite 13X/magnesium sulfate–water sorption thermal energy storage device for domestic heating," Energy Convers. Manag., vol. 171, no. January, pp. 98–109, 2018, doi: 10.1016/j.enconman.2018.05.077.

[8] P. Tatsidjodoung, N. Le Pierrès, J. Heintz, D. Lagre, L. Luo, and F. Durier, "Experimental and numerical investigations of a zeolite 13X/water reactor for solar heat storage in buildings," Energy Convers. Manag., vol. 108, pp. 488–500, 2016, doi: 10.1016/j.enconman.2015.11.011.

[9] S. Hongois, F. Kuznik, P. Stevens, and J. J. Roux, "Development and characterisation of a new MgSO4-zeolite composite for long-term thermal energy storage," Sol. Energy Mater. Sol. Cells, vol. 95, no. 7, pp. 1831–1837, Jul. 2011, doi: 10.1016/j.solmat.2011.01.050.

[10] S. P. Casey, D. Aydin, S. Riffat, and J. Elvins, "Salt impregnated desiccant matrices for 'open' thermochemical energy storage—Hygrothermal cyclic behaviour and energetic analysis by physical experimentation," Energy Build., vol. 92, pp. 128–139, Apr. 2015, doi: 10.1016/j.enbuild.2015.01.048.

[11] S. P. Casey, J. Elvins, S. Riffat, and A. Robinson, "Salt impregnated desiccant matrices for 'open' thermochemical energy storage—Selection, synthesis and characterisation of candidate materials," Energy Build., vol. 84, pp. 412–425, Dec. 2014, doi: 10.1016/j.enbuild.2014.08.028.

[12] G. Whiting, D. Grondin, S. Bennici, and A. Auroux, "Heats of water sorption studies on zeolite-MgSO4 composites as potential thermochemical heat storage materials," Sol. Energy Mater. Sol. Cells, vol. 112, pp. 112–119, May 2013, doi: 10.1016/j.solmat.2013.01.020.

[13] K. Johannes, F. Kuznik, J.-L. Hubert, F. Durier, and C. Obrecht, "Design and characterisation of a high powered energy dense zeolite thermal energy storage system for buildings," Appl. Energy, vol. 159, pp. 80–86, 2015, doi: 10.1016/j.apenergy.2015.08.109.

[14] V. M. van Essen et al., "Characterization of MgSO4 Hydrate for Thermochemical Seasonal Heat Storage," J. Sol. Energy Eng., vol. 131, 2009, doi: 10.1115/1.4000275.